J. Cent. South Univ. (2021) 28: 481−493
DOI: https://doi.org/10.1007/s11771-021-4616-y

Springer

Multi-objective capacity allocation optimization method of photovoltaic EV charging station considering V2G

ZHENG Xue-qin(郑雪钦), YAO Yi-ping(姚益萍)

School of Electrical Engineering and Automation, Xiamen University of Technology, Xiamen 361000, China

Abstract: Large-scale electric vehicles (EVs) connected to the micro grid would cause many problems. In this paper, with the consideration of vehicle to grid (V2G), two charging and discharging load modes of EVs were constructed. One was the disorderly charging and discharging mode based on travel habits, and the other was the orderly charging and discharging mode based on time-of-use (TOU) price; Monte Carlo method was used to verify the case. The scheme of the capacity optimization of photovoltaic charging station under two different charging and discharging modes with V2G was proposed. The mathematical models of the objective function with the maximization of energy efficiency, the minimization of the investment and the operation cost of the charging system were established. The range of decision variables, constraints of the requirements of the power balance and the strategy of energy exchange were given. NSGA-II and NSGA-SA algorithm were used to verify the cases, respectively. In both algorithms, by comparing with the simulation results of the two different modes, it shows that the orderly charging and discharging mode with V2G is obviously better than the disorderly charging and discharging mode in the aspects of alleviating the pressure of power grid, reducing system investment and improving energy efficiency.

Key words: vehicle to grid (V2G); capacity configuration optimization; time-to-use (TOU) price; multi-objective optimization; NSGA-II algorithm; NSGA-SA algorithm

Cite this article as: ZHENG Xue-qin, YAO Yi-ping. Multi-objective capacity allocation optimization method of photovoltaic EV charging station considering V2G [J]. Journal of Central South University, 2021, 28(2): 481−493. DOI: https://doi.org/10.1007/s11771-021-4616-y.

1 Introduction

With the widespread use of electric vehicles (EVs), the problem of the construction and planning of charging infrastructure brought by EV have drawn more and more attention from various countries [1]. At present, most of the energy for the primary side of the electric power system is still generated by coal, and the environmental pollution caused by EVs connected to the power grid through infrastructure is not lower than that of traditional cars. In order to solve this situation, we mainly adopt the following two approaches. Firstly, the renewable energy power generation system should be vigorously developed, and the absorption capacity of the power grid of renewable energy should be enhanced [2]. Secondly, the connection between renewable energy power generation system and charging facilities is directly established, which can realize the local consumption of renewable energy through micro-grid [3]. As the renewable energy has the characteristics of uncertain output, the second method is mainly used to optimize the capacity allocation of the micro-grid.

In addition, for EVs, using the V2G

Foundation item: Project(3502Z20179026) supported by Xiamen Science and Technology Project, China
Received date: 2020-06-11; **Accepted date:** 2020-11-20
Corresponding author: ZHENG Xue-qin, PhD, Professor; Tel: +86-15980859168; E-mail: 931152693@qq.com; ORCID: https://orcid.org/0000-0002-9075-5380

technology [4], the relatively reasonable time-of-use (TOU) price is established to attract the masses of the EV users through the charge and discharge of the distribution network to achieve for grid peak “cut”, which not only let the EV users to obtain certain benefits, but also can make the operation of the power grid be more stable [5, 6]. Therefore, in order to enable EV users to make better use of existing resources, it is particularly important to optimize the capacity allocation of charging stations [7].

The optimization of capacity allocation has been studied at home and abroad. LIU et al [8] took a typical independent microgrid as the research object, the multi-objective optimal capacity configuration model considering the economic efficiency, reliability, and environmental protection was established. Strength pareto evolutionary algorithm 2 (SPEA2) was proposed to solve the complex characteristics of the optimization model. The rationality and the effectiveness of the algorithm were further verified by an example. HUAN et al [9] presented a multi-objective optimization model for capacity optimization of solar and wind energy components in large-scale photovoltaic/wind power systems. The algorithm was used to solve the proposed model and obtain the exact solution. The results showed that the stability of wind power generation was more reliable than that of solar power generation. In Ref. [10], considering the uncertainty of load forecasting, market price errors and the uncertainties related to the variable output power of wind based distributed generation (DG) units, NSGA-II combined with fuzzy set theory is used to solve the combinatorial problem consisting of distribution system reconfiguration, capacitor allocation, and renewable energy resources sizing and siting simultaneously. In Ref. [11], a method of optimizing the storage capacity of direct current (DC) micro-grids considering the randomness of photovoltaic (PV) and load was proposed to maximize the local absorption of renewable energy. Based on the K-means algorithm, the engineering selection basis of PV and storage capacity in DC micro-grid system was given, and its economic benefit was evaluated.

However, the capacity configuration optimization problems that need to be considered when EVs with V2G behavior participate in the energy flow of charging stations have not been deeply analyzed in the most of the projects. Most studies only illustrated the advantages of the integrated approach in terms of the operation effect, economic benefit and network structure of the system in an integrated way, but failed to solve the optimization problem of each component unit in the charging station containing photovoltaic power generation system. Considering environmental and economic benefits comprehensively, in the planning of photovoltaic charging stations, the proportion of photovoltaic power generation in the charging energy of EVs should be increased as much as possible. On the other hand, the cost of construction and operation should be reduced as much as possible. At the current photovoltaic costs, the two are essentially contradictory. Therefore, the problem of multi-objective optimization should be solved.

Based on this, this paper first introduces two charging and discharging modes, and Monte Carlo method is used to simulate the charging and discharging load curves of the two modes. Secondly, under the two different charging and discharging modes, NSGA-II and NSGA-SA intelligent optimization algorithms are utilized to optimize the capacity configuration of photovoltaic charging stations. The results can provide a solution for the capacity configuration of the photovoltaic charging station to obtain the maximum energy efficiency with the lowest system cost.

2 System structure of photovoltaic charging station

The photovoltaic charging station studied in this paper includes central control unit, energy storage system, solar power generation system, charging and discharging parking space of EVs, multiple groups of DC/DC converter modules, AC/DC, DC/AC converter modules and converter distribution network modules, as shown in Figure 1.

3 EV charging and discharging load model

For the charging and discharging load mathematical mode of EVs entering the charging station of photovoltaic EVs, in order to reduce the load burden of the power grid, it is necessary to

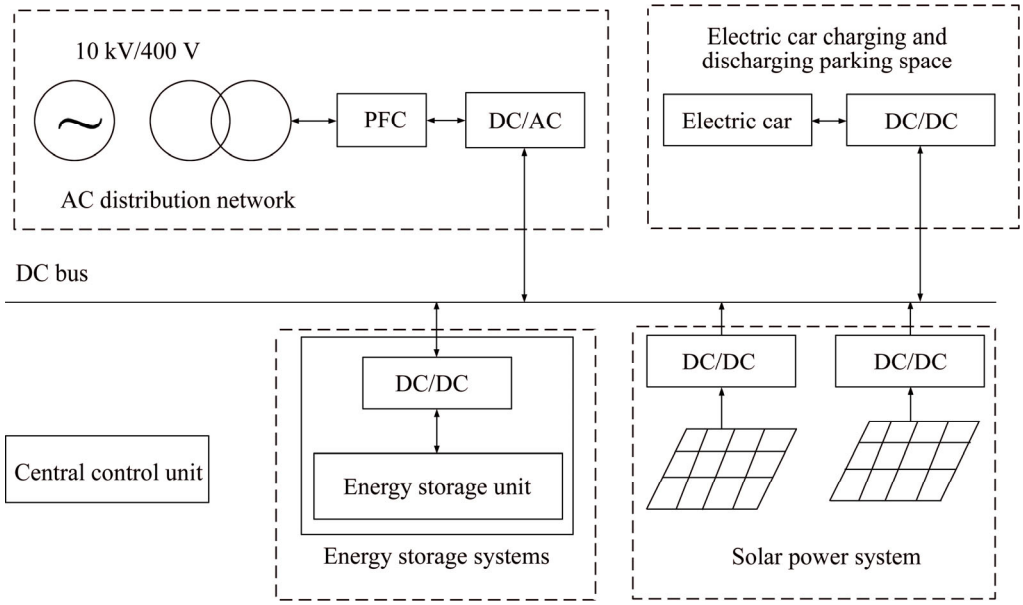

Figure 1 PV charging station system structure diagram

consider the "load shifting" for the power grid. In order to guide citizens to participate actively in the process, the corresponding policies should be made to enable citizens to get the maximum benefits in the process of participation. Therefore, the paper mainly takes private electric vehicle as the object of the research. Under the influence of TOU price of power grid, Monte Carlo method is adopted to simulate the daily load power curve of EVs.

3.1 Monte Carlo method

Monte Carlo method, or computer stochastic simulation method, is a calculation method based on random numbers. The flowchart of charge and discharge load calculation based on Monte Carlo method is shown in Figure 2.

3.2 Daily range of EVs

Generally, the daily mileage of private electric vehicles is mainly determined by users' behavior habits and daily needs. According to the US Department of Transportation survey of private electric vehicles in the United States in 2001, the daily mileage of EVs is approximately lognormal [12], and its probability density function, f_d, is shown in Eq. (1):

$$f_d = \frac{1}{\sqrt{2\pi}d\sigma_d}\exp\left[-\frac{(\ln d-\mu_d)^2}{2\sigma_d^2}\right] \quad (1)$$

where μ_d is the expected daily mileage, μ_d=3.2; σ_d is the standard deviation of daily mileage, σ_d=0.88;

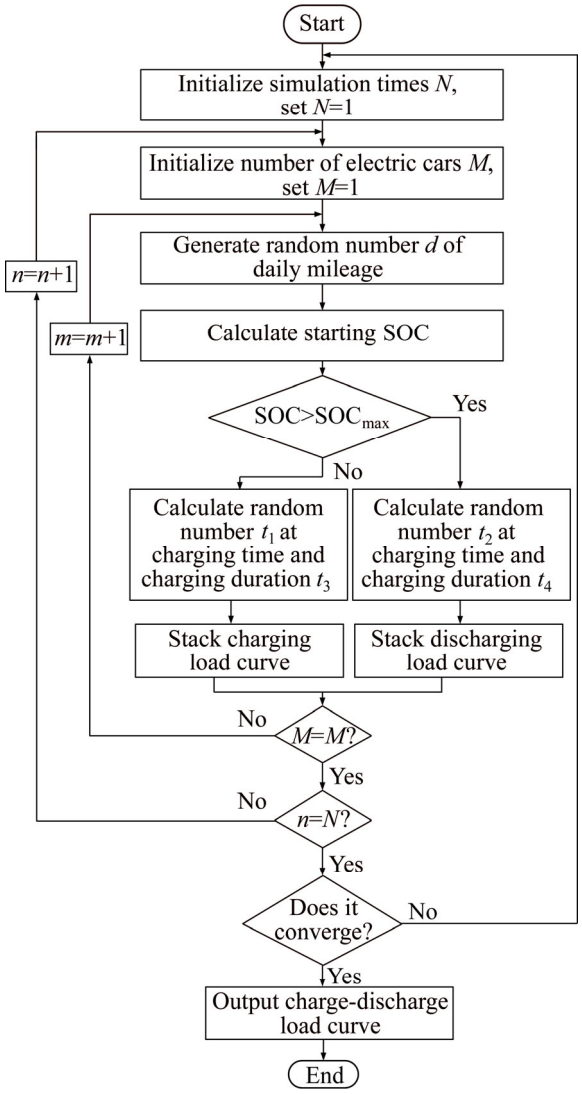

Figure 2 Flowchart of charge and discharge load calculation based on Monte Carlo method

d is the daily driving range of EVs, km.

Figure 3 shows the probability distribution of daily mileage of EVs.

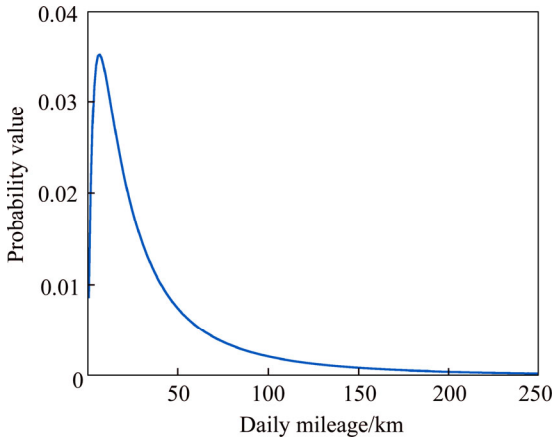

Figure 3 General distribution of daily mileage of EVs

3.3 Charging and discharging load model of EVs in disordered charging and discharging mode

3.3.1 Charging load model

Without consideration of TOU price, the EV starts to be charged after the return of the last trip. The initial SOC and the probability density function of the initial charging time [13] are as follows:

$$\mathrm{SOC}_1=\left(1-\frac{d}{d_\mathrm{m}}\right)\times 100\% \tag{2}$$

$$f_x(t_x)=\begin{cases}\dfrac{1}{\sqrt{2\pi}\sigma}\exp\left[-\dfrac{(t_x-\mu)^2}{2\sigma^2}\right], & \mu-12<t_x<24\\ \dfrac{1}{\sqrt{2\pi}\sigma}\exp\left[-\dfrac{(t_x+24-\mu)^2}{2\sigma^2}\right], & 0<t_x\le\mu-12\end{cases} \tag{3}$$

where d_m is the maximum daily driving range of the EV after it is fully charged; t_x is the starting time of charging; μ is the expected value of charging start time, μ=17.6; σ is the standard deviation of the start time of the charge, σ=3.4.

Assuming that the EV adopts the constant-current and constant-voltage charging mode, the charging duration time is as shown in Eq. (4):

$$t_1=\left(\frac{1-\mathrm{SOC}_1\times C_\mathrm{n}}{P_1\times k_1}\right) \tag{4}$$

where C_n is the capacity of lithium battery; P_1 is the charging power; $k1$ is the charging efficiency.

3.3.2 Discharging load model

It is assumed that EV starts to discharge as soon as it arrives at the charging station, and EV adopts the constant-current-constant-voltage discharge mode, and then the initial *SOC* [13] and duration of discharge are as follows:

$$\mathrm{SOC}_2=\left(1-\frac{d}{d_\mathrm{m}}\right)\times 100\% \tag{5}$$

$$t_2=\left(\frac{\mathrm{SOC}_1\times C_\mathrm{n}}{P_2\times k_2}\right) \tag{6}$$

where P_2 is the discharge power; k_2 is the discharge efficiency.

For the initial discharge time, it is assumed that the EV user arrives at the working point at 9 o'clock and leaves at 16 o'clock. It is also assumed that the EV parking at each time during the unit period is uniformly distributed. Then the probability density function [13] at the starting of discharge can be obtained, as shown in Eq. (7):

$$f_t(t_\mathrm{f})=\begin{cases}\dfrac{1}{7}, & t_\mathrm{f}\in[9,\ 16]\\ 0, & t_\mathrm{f}\in[0,\ 9)\cup(16,\ 24]\end{cases} \tag{7}$$

where t_f is the starting time of discharge.

3.4 Charging and discharging load model of EVs under orderly charging and discharging mode

3.4.1 TOU price mode

In order to improve the load curve in the peak and valley period of the power grid, the part of the load in the peak period will be transferred to the valley period. TOU price can be used to attract EV users to actively respond to the load shifting strategy. The mathematical model of TOU price [13] is as shown in Eq. (8):

$$\mathrm{Pr}(t)=\begin{cases}p_\mathrm{g}, & t\in[tg_1,\ tg_2]\\ p_\mathrm{f}, & t\in[tf_1,\ tf_2]\\ p_\mathrm{p}, & \text{otherwise}\end{cases} \tag{8}$$

where p_g, p_f, p_p are the valley price, peak price and peace price, respectively, and $p_\mathrm{g}<p_\mathrm{p}<p_\mathrm{f}$; tf_1, tf_2 are the beginning and end of peak electricity price, respectively; tg_1, tg_2 are the beginning time of valley electricity price and the end time of valley electricity price, respectively; the rest of the time is flat price.

3.4.2 Charging load model

Assuming that the daily mileage of private electric vehicles is not affected by TOU price, the charging time of owners who respond to TOU price [13] is as shown in Eq. (9):

$$t_{sc}=\begin{cases}t_{g1}+\text{rand}(\Delta t_1-t_c),\ 0\le t_c\le\Delta t_1\\ t_{g1},\ t_c>\Delta t_1\end{cases} \tag{9}$$

where t_{sc} is the charging time of private electric vehicles in TOU price mode; rand( ) is the random number in the interval of [0, 1]; t_{g1} is the starting time of valley electricity price; t_{g2} is the end time of valley electricity price; Δt_1 is the duration of valley electricity price, $\Delta t_1=tg_2-tg_1$.

3.4.3 Discharge load model

In order to make the owner obtain more benefits in the peak and valley segment as far as possible, the initial discharge time of the owner who responds to TOU price [13] is as shown in Eq. (10):

$$t_{sd}=\begin{cases}t_{f1}+\text{rand}(\Delta t_2-t_d),\ 0\le t_d\le\Delta t_2\\ t_{f1},\ t_d>\Delta t_2\end{cases} \tag{10}$$

where t_d is the starting discharge time of private electric vehicles under TOU price mode; t_{f1} is the starting time of peak electricity price; t_{f2} is the end time of peak electricity price; Δt_2 is the duration of peak electricity price, $\Delta t_2=tf_2-tf_1$.

3.4.4 Charging and discharging load calculation of EVs in different charging and discharging modes

In order to calculate the load model of EVs under the above two charging and discharging modes, it is assumed that the number of private electric vehicles entering the photovoltaic charging station on a certain day is one hundred. The parameters of the private electric vehicles are as follows. Lithium battery capacity is 35 kW·h, within a day of conventional charging and discharging, the fast charging and discharging mode, and fast charge power is 28 kW. The fast charging efficiency is 0.9, and fast discharge power is 20 kW. The fast discharge efficiency is 0.85. Every hundred kilometers power consumption quantity is 20 kW·h. Monte Carlo method is used to simulate the charging and discharging load models of the EVs entering the charging station.

The charging and discharging power of EVs at each moment in the disorderly charging and discharging mode can be obtained, as shown in Figure 4.

Under the disorderly charging and discharging model, the charging power is positive and the discharging power is negative. From the load curve, under the state of EV charging, the charging load of

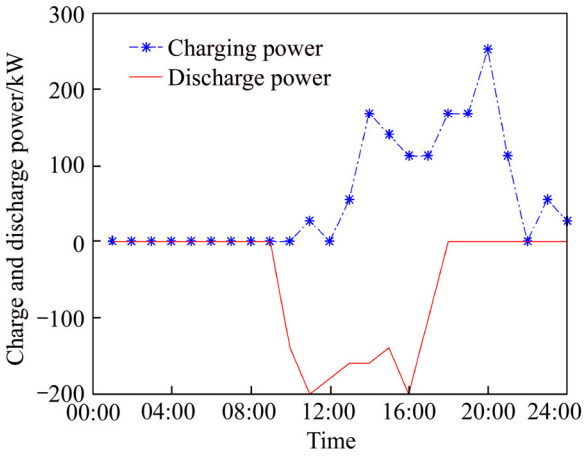

Figure 4 Charging and discharging power of EV at each moment under disorderly charging and discharging mode

the private electric vehicles starts to rise at 10 o'clock. That is, EVs gradually enter the charging station for charging. At 20 o'clock, the charging power reaches the maximum, and the maximum charging load is about 250 kW. Meanwhile, at 13−21 o'clock, most EVs enter the charging station for charging. At 11 and 16 o'clock, the discharge power reaches the maximum, and the maximum discharge load is about 200 kW. At the same time, from 10 to 17 o'clock, most of the EVs enter the charging station and discharge.

The charging and discharging powers of EVs at each moment under the orderly charging and discharging mode are shown in Figure 5.

Under the orderly charging and discharging mode, the charging power is positive and the discharge power is negative. From the load curve, in the charging state of EV, private electric vehicles mainly enter the charging station at 0−10 o'clock

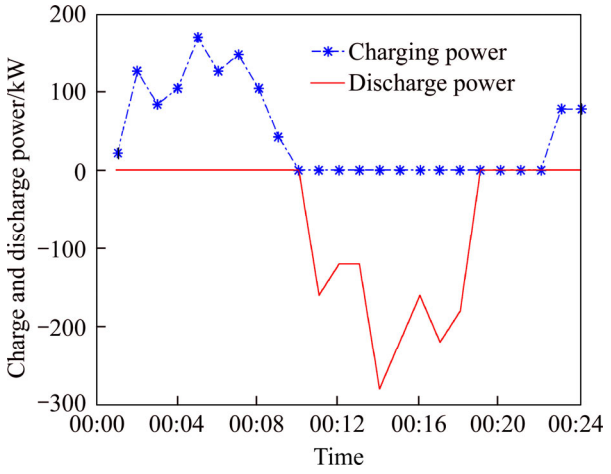

Figure 5 Charging and discharging power of EVs at each moment under orderly charging and discharging mode

and 22−24 o'clock, and the maximum charging load is about 180 kW. Under the state of EV discharge, private electric vehicles mainly discharge at the charging station from 10−19 o'clock, and the maximum discharge load is about 290 kW.

Through the above comparison, it can be seen that under the disorderly charging and discharging model, the charging load is mainly concentrated at the time of 13−21 o'clock. But this time is also the peak period of power consumption of the power grid, which undoubtedly increases the burden on the power grid. In the orderly charging and discharging mode, the charging load is mainly concentrated in the low period of power consumption, namely 0−10 and 22−24 o'clock. The maximum charging load under the disorderly charging and discharging model is nearly 70 kW more than that under TOU price which is adverse to the optimization of system capacity configuration. Therefore, under the orderly charging and discharging mode, the charging and discharging power of EVs at each moment can better play the role of load shifting for the distribution network.

4 Mathematical model of capacity allocation optimization

4.1 Multi-objective evolutionary algorithm NSGA-II

Multi-objective evolutionary algorithm NSGA-II is an algorithm that adopts both elite retention strategy and multiple protection methods [14, 15]. The performance and the efficiency are better than traditional evolutionary algorithm. This method not only reduces the computational complexity, but also has the characteristics of fast operation and good convergence of solution set. The flowchart of solving the model based on NSGA-II optimization algorithm is shown in Figure 6.

4.2 Multi-objective evolutionary algorithm NSGA-SA

The local searching ability of the genetic algorithm is not strong and easy to fall into the local optimal solution. While simulated annealing algorithm can effectively avoid falling into the local optimal solution during the search process. A hybrid algorithm (NSGA-SA) with good convergence and stability can be obtained by combining the genetic algorithm with the simulated annealing algorithm [16]. The flowchart of solving the model based on NSGA-SA optimization algorithm is shown in Figure 7.

4.3 Objective function

Under the premise of satisfying the demand of charging and discharging in the station, the designed objective functions [17] are as follows: the total investment of the system and the minimum operation cost, most energy efficient are as shown in Eq. (11):

$$\begin{cases} \min C_{\Sigma} = \min(C_{\mathrm{pv}} + C_{\mathrm{b}} + C_{\mathrm{dc1}} + C_{\mathrm{dc2}} + \\ \quad C_{\mathrm{dc3}} + C_{\mathrm{ad}} + C_{\mathrm{g}}) \\ \max \mathrm{EUR} = \max \dfrac{\int_0^{8760} (P_{n1}(t) - P_{g1}(t))\mathrm{d}t}{\int_0^{8760} P_{n1}(t)\mathrm{d}t} \times 100\% \end{cases} \tag{11}$$

where C_{Σ} is the total cost of the system; C_{pv}, C_{b}, C_{dc1}, C_{dc2}, C_{dc3}, C_{ad}, C_{g} are the total cost of solar panels, total cost of energy storage module, total cost of photovoltaic converter module, total cost of charging module, total cost of energy storage converter module, total cost of grid-connected converter module and total electricity charge purchased from the power grid, respectively [17]; $P_{n1}(t)$, $P_{g1}(t)$ is the charging power of the EV and the power absorbed from the grid at time, respectively.

$$C_{\mathrm{pv}} = N_{\mathrm{pv}} C_{\mathrm{a}} \frac{r_0(1+r_0)^m}{(1+r_0)^m - 1} + a \tag{12}$$

$$C_{\mathrm{b}} = \left[N_{\mathrm{b}} C_{\mathrm{b}} \frac{r_0(1+r_0)^m}{(1+r_0)^m - 1} + d1 \right] + b \tag{13}$$

$$C_{\mathrm{dc1}} = N_{\mathrm{dc1}} C_{\mathrm{c}} \frac{r_0(1+r_0)^m}{(1+r_0)^m - 1} + cN_{\mathrm{dc1}} \tag{14}$$

$$C_{\mathrm{dc2}} = N_{\mathrm{dc2}} C_{\mathrm{d}} \frac{r_0(1+r_0)^m}{(1+r_0)^m - 1} + dN_{\mathrm{dc2}} \tag{15}$$

$$C_{\mathrm{dc3}} = N_{\mathrm{dc3}} C_{\mathrm{e}} \frac{r_0(1+r_0)^m}{(1+r_0)^m - 1} + eN_{\mathrm{dc3}} \tag{16}$$

$$C_{\mathrm{ad}} = N_{\mathrm{ad}} C_{\mathrm{f}} \frac{r_0(1+r_0)^m}{(1+r_0)^m - 1} + fN_{\mathrm{ad}} \tag{17}$$

$$C_{\mathrm{g}} = C_{\mathrm{g1}} \int_0^{8760} \left[P_{\mathrm{g}}(t) - P_{n2}(t) \right] \mathrm{d}t \tag{18}$$

where N_{pv}, N_{b}, N_{dc1}, N_{dc2}, N_{dc3}, N_{ad} are the number of solar panels, energy storage cells, photovoltaic

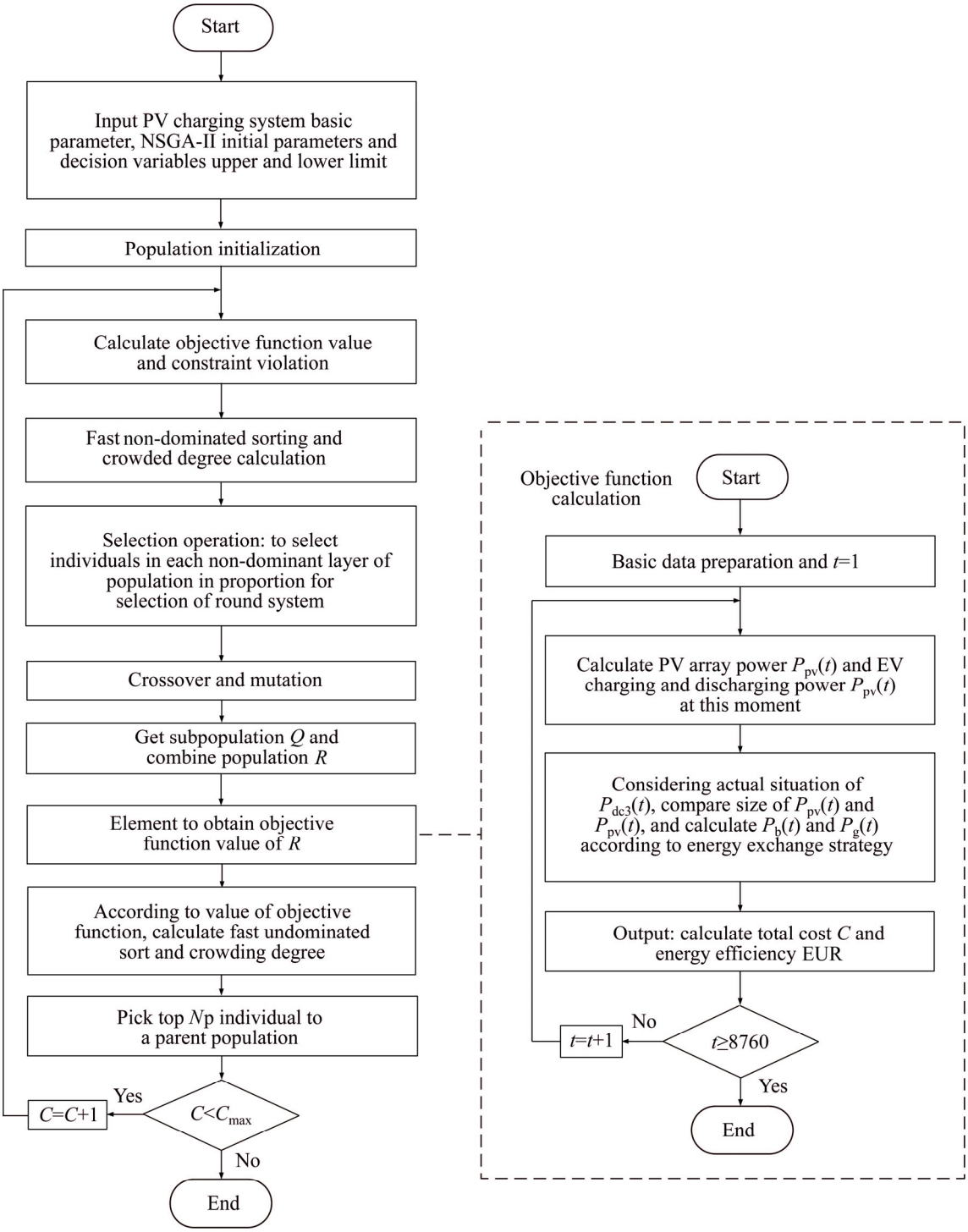

Figure 6 Flowchart of solving model based on NSGA-II optimization algorithm

converter modules, charging and discharging modules, energy storage converter modules and grid-connected converter modules, respectively; C_a, C_b, C_c, C_d, C_e, C_f, C_g are the unit price of solar panel, energy storage cell, photovoltaic converter module, charging module, energy storage converter module, grid-connected converter module and price of purchasing power from grid, respectively; a, b, c, d, e, f are the unit prices of corresponding maintenance and operation costs; m is the system life; r_0 is the discount rate; d is the proportion of energy of energy storage battery eliminated each year in total energy storage; $P_{n1}(t)$, $P_{n2}(t)$ are the power absorbed and released by the EV to the distribution network and the power released by the EV to the charging station, respectively.

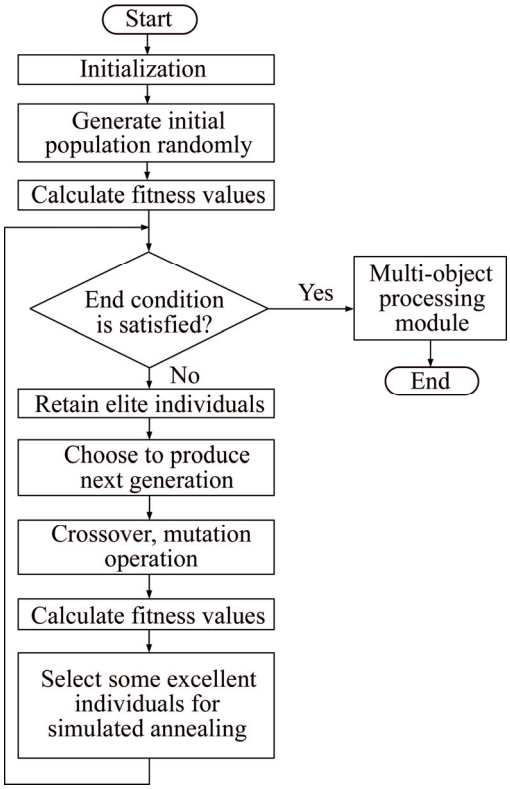

Figure 7 Flowchart of solving model based on NSGA-SA optimization algorithm

4.4 Constraints

4.4.1 Constraints for each decision variable

For a certain city, the annual sunshine pattern and the distribution of charging and discharging power demand are fixed each year. Therefore, the decision-making variables of the photovoltaic charging station system are as follows: PV module inclination θ, solar panels number N_{pv}, PV converter modules number N_{dc1}, charging modules number N_{dc2}, energy storage converter modules number N_{dc3}, energy storage battery number N_{b}, sunshine percentage S, and ambient temperature T.

$$\begin{cases} 0° \le \theta \le 90° \\ 0 < N_{\text{pv}} \le N_{\text{pv.max}} \\ 0 \le N_{\text{dc1}} \le N_{\text{dc1.max}} \\ 0 \le N_{\text{dc2}} \le N_{\text{dc2.max}} \\ 0 \le N_{\text{dc3}} \le N_{\text{dc3.max}} \\ 0 \le N_{\text{b}} \le N_{\text{b.max}} \\ 0 \le N_{\text{ad}} \le N_{\text{ad.max}} \\ 0 \le S \le 1 \\ 0° \le T \le 40\ °\text{C} \end{cases} \tag{19}$$

where types of $N_{\text{pv.max}}$, $N_{\text{dc1.max}}$, $N_{\text{dc2.max}}$, $N_{\text{dc3.max}}$, $N_{\text{b.max}}$, $N_{\text{ad.max}}$ are determined by the actual situation.

4.4.2 Power balance constraint that satisfies charging and discharging requirements

At any time t, the PV power $P_{\text{pv}}(t)$ absorbed by the charging station system, charging and discharging power $P_{n1}(t)$, $P_{n2}(t)$, energy storage charging discharge power $P_{\text{b}}(t)$, absorbing power $P_{g1}(t)$ from the distribution network and releasing power $P_{g2}(t)$ are in equilibrium.

When the energy storage battery is in charging state:

$$P_{\text{pv}}(t)X_{\text{pv}} + P_{n2}(t)/X_{\text{dc2}} = P_{n1}(t)/X_{\text{dc2}} + P_{\text{b}}(t)/X_{\text{dc3}}.$$

When the energy storage battery is in discharging state:

$$P_{n1}(t)/X_{\text{dc2}} = P_{\text{pv}}(t)X_{\text{dc1}} + P_{\text{b}}(t)/X_{\text{dc3}} + P_{n2}(t)/X_{\text{dc2}}.$$

4.5 Mathematical model of energy exchange strategy

The power balance relationship of the system should meet the following requirements.

4.5.1 Energy storage system in charging state

1) $N_{\text{dc3}}P_{\text{dc3}} \ge P_{\text{pv}}(t)X_{\text{pv}} + P_{n2}(t)/X_{\text{dc2}} - P_{n1}(t)/X_{\text{dc2}}$, that is, when the sum of the photovoltaic power and the power released by the EV to the charging station is only enough to provide charging power to the energy storage system, the charging power of the energy storage system and the absorbed power to the distribution network are shown as follows:

$$\begin{cases} P_{\text{b}}(t) = (P_{\text{pv}}(t)X_{\text{pv}} + P_{n2}(t)/X_{\text{dc2}} - P_{n1}(t)/X_{\text{dc2}})X_{\text{dc3}} \\ P_{\text{g}}(t) = 0 \end{cases}$$

2) $N_{\text{dc3}}P_{\text{dc3}} < P_{\text{pv}}(t)X_{\text{pv}} + P_{n2}(t)/X_{\text{dc2}} - P_{n1}(t)/X_{\text{dc2}}$, that is, the sum of the photovoltaic power and the power released by the EV to the charging station can be supplied to the energy storage system for charging, and then the residual energy can be supplied to the power grid. At this time, the charging power of the energy storage system and the absorbed power to the distribution network are shown as follows:

$$\begin{cases} P_{\text{b}}(t) = N_{\text{dc3}}P_{\text{dc3}} \\ P_{\text{g}}(t) = -(P_{\text{pv}}(t)X_{\text{pv}} + P_{n2}(t)/X_{\text{dc2}} - P_{n1}(t)/X_{\text{dc2}} - \\ \qquad P_{\text{b}}(t)/X_{\text{dc3}})X_{\text{ad}} \end{cases}$$

4.5.2 Energy storage system in discharge state

1) $N_{\text{dc3}}P_{\text{dc3}} \ge P_{n1}(t)/X_{\text{dc2}} - P_{\text{pv}}(t)X_{\text{pv}} - P_{n2}(t)/X_{\text{dc2}}$, that is, when the power of energy storage system and photovoltaic power generation can meet the charging demand of EV, the charging power of the

energy storage system and the absorbed power to the distribution network are shown as follows:

$$\begin{cases} P_{\mathrm{b}}(t)=-(P_{n1}(t)/X_{\mathrm{dc2}}-P_{\mathrm{pv}}(t)X_{\mathrm{pv}}-P_{n2}(t)/X_{\mathrm{dc2}})X_{\mathrm{ad}} \\ P_{\mathrm{g}}(t)=0 \end{cases}$$

2) $N_{\mathrm{dc3}}P_{\mathrm{dc3}}<P_{n1}(t)/X_{\mathrm{dc2}}-P_{\mathrm{pv}}(t)X_{\mathrm{pv}}-P_{n2}(t)/X_{\mathrm{dc2}}$, that is, when the energy storage system does not discharge, and the photovoltaic power is insufficient to meet the charging demand of EV, the charging power of the energy storage system and the absorbed power to the distribution network are shown as follows:

$$\begin{cases} P_{\mathrm{b}}(t)=0 \\ P_{\mathrm{g}}(t)=(P_{n1}(t)/X_{\mathrm{dc2}}-P_{\mathrm{pv}}(t)X_{\mathrm{pv}}-P_{n2}(t)/X_{\mathrm{dc2}})X_{\mathrm{ad}} \end{cases}$$

5 Example analysis

To verify the above algorithms and optimization model, in a certain area (115°43′E, 36°30′N), taking an area of 2000 m^2 of PV charging station planning as an example, the capacity allocation optimization, including solar panels, can provide the maximum power of 220 kW. The formula of radiation amount in this region can be quoted from Refs. [18, 19], and the power of photovoltaic modules in this region can be quoted from Ref. [20]. The optimization model, NSGA-II and NSGA-SA algorithm are programmed and solved by software MATLAB. In the program, the population number N_{p} is set to 100; the maximum number of iterations is 200; the crossover probability is 0.9; and the mutation probability is 0.1. The photovoltaic charging station is equipped with 80 charging piles. Conventional charging methods are adopted. The rated power of a single charging pile is 10 kW. The rated capacity of the battery is 1000 kW·h, and the maximum discharge depth is 70%. The rated power of the DC-DC converter module is 200 kW. Both AC-DC and DC-AC converter modules are rated at 560 kW.

The upper and lower limits for the decision variables should be determined according to the actual situation. For a photovoltaic charging station, the upper limit of the decision variables, θ, N_{pv}, N_{dc1}, N_{dc2}, N_{dc3}, N_{b}, S, T are respectively π/2, 2500, 100, 36, 25, 100, 1, 40 °C. The lower limit are 0°, 0, 0, 0, 0, 0, 0 °C. The other system parameters are shown in the attached table in the appendix. The system is simulated and solved to obtain the Pareto optimal solution frontier under different charging and discharging modes of EVs, as shown in Figure 8.

The Pareto solution set can provide decision-makers with much useful information on energy efficiency and system investment, operation cost, which are in conflict with each other. Therefore, in order to make more objective and more comprehensive decisions, decision makers need to consider all aspects of factors comprehensively and fully dig out the information contained in Pareto.

As can be seen from Figure 8, the total investment and operation cost of the system increase with the increase of energy efficiency, and the two objects cannot reach to the optimal value at the same time. Based on the NSGA-II algorithm, by comparing the optimization results under the two modes, the energy efficiency under the orderly charging and discharging mode is higher than that under the disorderly charging and discharging mode under the same total investment of the system and operating cost, and the energy is more fully utilized. This indicates that under the orderly charging and discharging mode, energy efficiency is not only improved, but also the total investment of the system and the operating cost are reduced, which will bring more benefits to the charging station. In order to further verify the conclusion, NSGA-SA algorithm is added as a comparison to prove the reliability of the above results.

In addition, in the same mode, comparing with NSGA-II, NSGA-SA the same energy efficiency can be achieved by using fewer modules and costs . However, the obtained solution set is relatively scatter, and it is basically concentrated in low energy utilization and low cost areas.

Simulation of the system can be obtained as shown in Table 1 (disorderly charging and discharging mode is based on NSGA-II), Table 2 (the orderly charging and discharging mode is based on NSGA-II), Table 3 (disorderly charging and discharging mode is based on NSGA-SA), Table 4 (the orderly charging and discharging mode is based on NSGA-SA) capacity configuration optimization scheme.

From the above table, the values of the parameters of each variable of the system can be obtained under the condition of different energy efficiency of the charging station, so as to provide data reference for the capacity configuration of the charging station. Based on NSGA-II and NSGA-SA

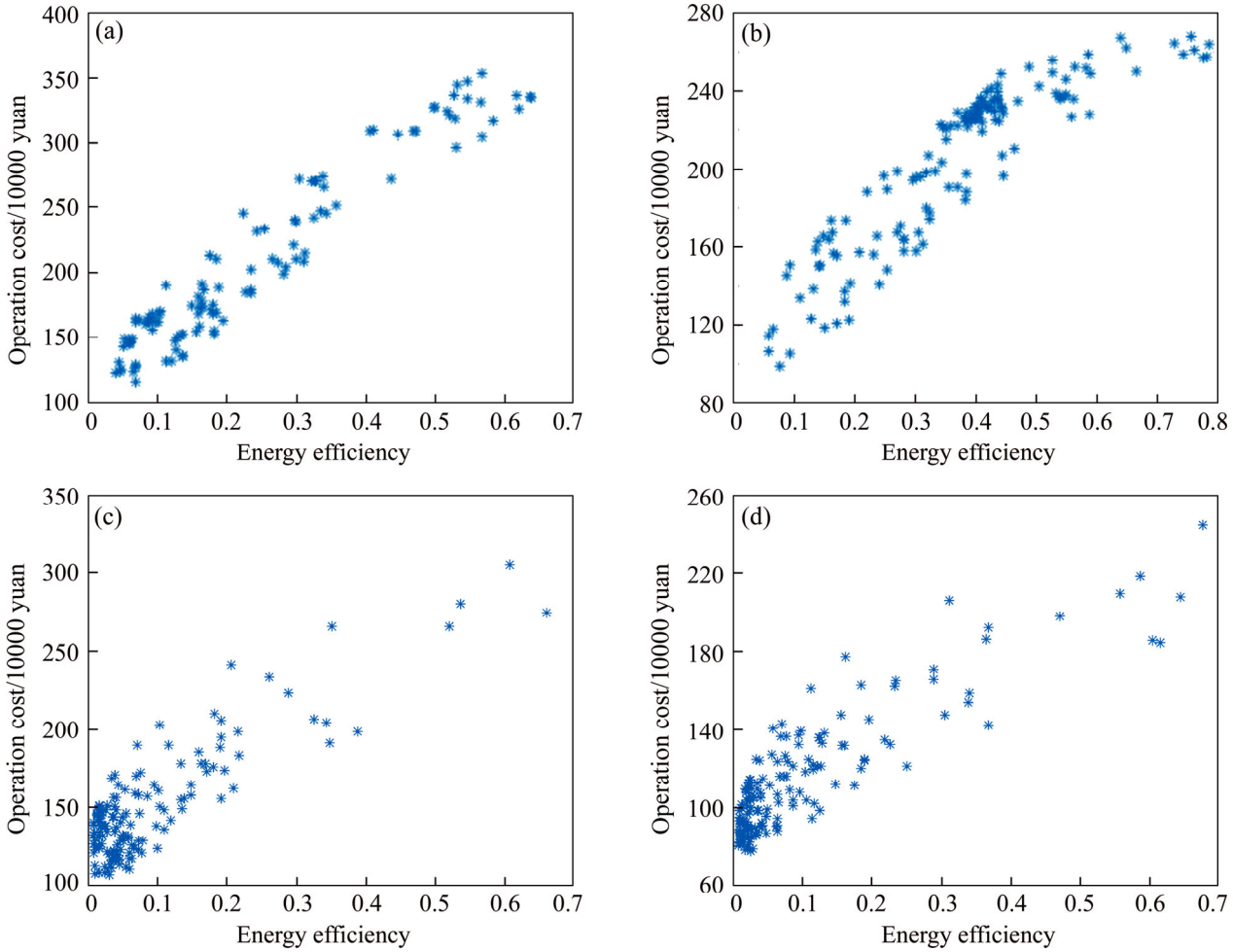

Figure 8 Pareto optimal solution frontier under different charging and discharging modes: (a) NSGA-II two-objective optimization results (disorderly charging and discharging mode); (b) NSGA-II two-objective optimization results (orderly charging and discharging mode); (c) NSGA-SA two-objective optimization results (disorderly charging and discharging mode); (d) NSGA-SA two-objective optimization results (orderly charging and discharging mode)

Table 1 Optimum solutions (disorderly charging and discharging mode is based on NSGA-II)

Parameter		The best angle/(°)	Number of photovoltaic cells	Number of photovoltaic converter modules	Number of charge and discharge modules	Number of energy storage and converter modules	Number of energy storage batteries	Sunshine percentage	Cost/ 10000 yuan	Temperature/ °C
EUR	10%	39.49	665.00	29.00	7.00	7.00	38.00	0.31	136.54	39.30
	30%	39.49	1643.00	55.00	13.00	15.00	60.00	0.37	240.04	30.40
	50%	39.49	2463.00	86.00	24.00	21.00	92.00	0.65	304.48	17.70

Table 2 Optimum solutions (orderly charging and discharging mode is based on NSGA-II)

Parameter		The best angle/(°)	Number of photovoltaic cells	Number of photovoltaic converter modules	Number of charge and discharge modules	Number of energy storage and converter modules	Number of energy storage batteries	Sunshine percentage	Cost/ 10000 yuan	Temperature/ °C
EUR	10%	39.49	553.00	22.00	10.00	5.00	34.00	0.31	99.12	37.30
	30%	39.49	1526.00	47.00	19.00	12.00	54.00	0.37	195.49	27.30
	50%	39.49	2358.00	76.00	29.00	17.00	87.00	0.65	242.12	16.10

Table 3 Optimum solutions (disorderly charging and discharging mode is based on NSGA-SA)

Parameter		The best angle/(°)	Number of photovoltaic cells	Number of photovoltaic converter modules	Number of charge and discharge modules	Number of energy storage and converter modules	Number of energy storage batteries	Sunshine percentage	Cost/ 10000 yuan	Temperature/ °C
	10%	38.26	650	27	6	6	35	0.21	123.97	39.2
EUR	30%	38.26	1532	50	12	13	59	0.25	206.87	30.1
	50%	38.26	2371	83	22	21	90	0.49	280.30	17.9

Table 4 Optimum solutions (orderly charging and discharging mode is based on NSGA-SA)

Parameter		The best angle/(°)	Number of photovoltaic cells	Number of photovoltaic converter modules	Number of charge and discharge modules	Number of energy storage and converter modules	Number of energy storage batteries	Sunshine percentage	Cost/ 10000 yuan	Temperature/ °C
	10%	38.29	548.00	21.00	9.00	4.00	32.00	0.21	98.52	37.10
EUR	30%	38.29	1432.00	43.00	18.00	12.00	50.00	0.25	171.23	26.90
	50%	38.29	2270.00	73.00	27.00	16.00	82.00	0.49	218.11	15.80

algorithms, in the orderly charging and discharging mode, the number of photovoltaic cells, photovoltaic converter module, as well as the energy storage battery and energy storage cells decreases, while the number of energy storage conversion modules increases. The results show that by comparing with the disorderly charging and discharging mode, this mode can provide more energy for EV charging and reduce the cost. Moreover, it can be seen that the number of devices used in the orderly charging and discharging mode is less than that in the disorderly charging and discharging mode. Because in the orderly charging and discharging mode, EVs can provide more energy to the grid during the peak period of the grid's power consumption, which can reduce the number of photovoltaic cells and photovoltaic converter modules. At this time, the grid is just at the peak of the power consumption. Therefore, the energy supplied by the EVs to the grid can be directly transmitted to the grid for secondary use without having to store it in the energy storage battery, so the number of energy storage batteries and energy storage converter modules is also reduced. Moreover, under the same energy efficiency, the simulation results using NSGA-SA algorithm are better than that using NSGA-II. From the above factors, the scheme under the orderly charging and discharging mode with V2G is more suitable for the capacity configuration optimization of photovoltaic charging stations.

6 Conclusions

In this paper, the load models of two different charging and discharging modes with V2G are firstly constructed. Due to insufficient consideration of the travel habits of EV users, the disorderly charging and discharging mode has not been established corresponding to the TOU price mode. As a result, parking time is free for travelers, but the corresponding user cost is also increased. The Monte Carlo method is used to simulate the example to verify that the orderly charging and discharging model can play a better role in "peak-load shifting" for the power grid. Two multi-objective optimization algorithms are introduced. Through the introduction of energy exchange strategy and the establishment of objective function, the mathematical models of photovoltaic charging station capacity allocation optimization are established. Finally, an example is given to verify that under the comparison between two different algorithms and two different charging and discharging modes. The optimization results of NSGA-SA are better than NSGA-II. However, the solution sets are relatively dispersed, most of which focused on low cost and low energy efficiency, which can not well represent the high cost and energy efficiency. In conclusion, from the above comparison, the orderly charging and discharging with V2G can bring the maximum benefits to the grid and reduce the power consumption pressure.

Nomenclature

Solar panel unit price, C_a/(10000 yuan·kW^{-1})	0.04
PV battery life, m/year	20
PV array efficiency, X_{pv}/%	21
PV converter module (single-track DC/DC) rated power, P_{pv}/kW	10
Photovoltaic converter module Price, C/10000 yuan	0.95
Price of energy storage battery, C_b/(10000 yuan·kW^{-1})	0.3
Energy storage and variable current module price, C_e/10000 yuan	1.2
Rated power P_b/kW of energy storage and converter module (bidirectional DC/DC)	10
Efficiency of energy storage and converter Module X_{dc2}/%	90
Charge and discharge module price C_d/10000 yuan	2
Power battery charging and discharging module (bidirectional DC/DC) rated power P_b/kW	10
Efficiency of charging and discharging modules, X_{dc3}/%	93
Grid-connected converter module C_f/(10000 yuan·kW^{-1})	0.95
Grid-connected converter module Efficiency X_{ad}/%	91
Discount rate, r_0	0.06

Contributors

ZHENG Xue-qin provided the general research direction of the paper and revised the paper. YAO Yi-ping collected data, built models and wrote the original paper. All authors replied to reviewers' comments and revised the final version.

Conflict of interest

ZHENG Xue-qin and YAO Yi-ping declare that they have no conflict of interest.

References

[1] ZEFREH M S, TODD T D, KARAKOSTAS G. Energy provisioning and operating costs in hybrid solar-powered infrastructure [J]. IEEE Transactions on Sustainable Energy, 2014, 5(3): 986−994. DOI: 10.1109/TSTE.2014.2319239.

[2] AI-OGAILI A S, HASHIM T J T, TAHMAT N A, RAMASAMY A K, MARSADEK M B, FAISAL M, HANNAN M A. Review on scheduling, clustering, and forecasting strategies for controlling electric vehicle charing: Challenges and recommendations [J]. IEEE Access, 2019, 7: 128353−128371. DOI: 10.1109/ACCESS.2019.2939595.

[3] LIU Jian-zhe, CHEN Hua, ZHANG Wei, YURKOVICH B, RIZZONI G. Energy management problems under uncertainties for grid-connected microgrids: A chance constrained programming approach [J]. IEEE Transactions on Smart Grid, 2017, 8(6): 2585−2596. DOI: 10.1109/TSG.2016.2531004.

[4] SAINS N S, AI-ANBAGI I. Optimal charging and discharging for EVs in a V2G participation under critical peak conditions [J]. IET Electrical Systems in Transportation, 2018, 8(2): 136−143. DOI: 10.1049/iet-est.2017.0073.

[5] YANG He-jun, WANG Lei, ZHANG Ye-yu, TAI Heng-ming, MA Ying-hao, ZHOU Ming. Reliability evaluation of power system considering time of use electricity pricing [J]. IEEE Transactions on Power Systems, 2019, 34(3): 1991−2002. DOI: 10.1109/TPWRS.2018.2879953.

[6] LIU Xiao-ling, WANG Zhao-jie, GAO Feng, WU Jiang, GUAN Xiao-hong, ZHOU Dian-min. Response behaviors of power generation and consumption in energy intensive enterprise under time-of-use price [J]. Power System Automation, 2014(8): 41−49. DOI: 10.7500/AEPS20130502007. (in Chinese)

[7] YANG Hong-ming, YANG Song-ping, XU Yan, CAO Er-bao, LAI Ming-yong, ZHAO Yang-dong. Electric vehicle route optimization considering TOU electricity price by learnable partheno-genetic algorithm [J]. IEEE Transactions on Smart Grid, 2015, 6(2): 657−666. DOI: 10.1109/TSG.2014.2382684.

[8] LIU Hui-wen, WANG Sheng-tie, LIU Guang-chen, ZHANG Jian-wei, WEN Su-fang. SARAP algorithm of multi-objective optimal capacity configuration for WT-PV-DE-BES Stand-Alone Microgrid [J]. IEEE Access, 2020, 8: 126825−126838. DOI:10.1109/ACCESS.2020.3008553.

[9] HUAN Long, MEHRDAD E, ZHANG Zi-jun. Configuration optimization and analysis of a large scale PV/Wind system [J]. IEEE Transactions on Sustainable Energy, 2017, 8(1): 84−93. DOI: 10.1109/TSTE.2016.2583469.

[10] RAVADANEGH S N, OSKUEE M R, KARIMI M. Multi-objective planning model for simultaneous reconfiguration of power distribution network and allocation of renewable energy resources and capacitors with considering uncertainties [J]. Journal of Central South University, 2017, 24(8): 1837−1849. DOI: 10.1007/s11771-017-3592-8.

[11] WU Ming, SUN Li-jing, ZHANG Hai, WANG Wei, LUO Guo-min. Research on optimal storage capacity of DC micro-grid system in PV station [J]. The Journal of Engineering, 2017, 2017(13): 859−864. DOI: 10.1049/joe.2017.0452.

[12] TAYLOR M J, ALEXANDER A. Evaluation of the impact of plug-in electric vehicle loading on distribution system operations [C]// IEEE Power & Energy Society General Meeting. Calgary, 2009: 1−6. DOI: 10.1109/PES.2009.5275317.

[13] XU Shan, LI Yang. An optimization model of peak-valley price time interval for guiding the orderly charging

and discharging of electric vehicles [J]. Power Demand Side Management, 2018, 20(5): 11−15. DOI: 10.3969/j.issn.1009-1831.2018.05.003. (in Chinese)

[14] AKBARI M, SHOJAEEFARD M H, ASADI P, KHALKHALI A. Hybrid multi-objective optimization of microstructural and mechanical properties of B_4C/A356 composites fabricated by FSP using TOPSIS and modified NSGA-II [J]. Transactions of Nonferrous Metals Society of China, 2017, 27(11): 2317−2333. DOI: 10.1016/S1003-6326(17)60258-9.

[15] SU Chun, LIU Yang. Multi-objective imperfect preventive maintenance optimisation with NSGA-II [J]. International Journal of Production Research, 2020, 58(13): 4033−4049. DOI: 10.1080/00207543.2019.1641237.

[16] WANG Lan, LI Xin-hua. Study of distortion correction of bp neural network based on improved genetic simulated annealing algorithm [J]. Computer Measurement and Control, 2019, 27(5): 77−81. DOI: 10.16526/j.cnki.11-4762/tp.2019.05.018. (in Chinese)

[17] LU Xin-yi, LIU Nian, CHEN Zheng, ZHANG Jian-hua, XIAO Xiang-ning. Multi-objective optimal scheduling for PV-Assisted charging of electric vehicles [J]. Transactions of China Electrotechnical Society, 2014, 29(8): 46−56. DOI: 10.3969/j.issn.1000-6753.2014.08.006. (in Chinese)

[18] MA R, LETU H, YANG K, WANG T, CHEN L. Estimation of surface shortwave radiation from himawari-8 satellite data based on a combination of radiative transfer and deep neural network [J]. IEEE Transactions on Geoscience and Remote Sensing, 2020, 58(8): 5304−5316. DOI: 10.1109/TGRS.2019.2963262.

[19] ALSADI S Y, NASSAR Y F. Estimation of solar irradiance on solar fields: An analytical approach and experimental results [J]. IEEE Transactions on Sustainable Energy, 2017, 8(4): 1601−1608. DOI: 10.1109/TSTE.2017. 2697913.

[20] YU Dong-xia, ZHANG Jian-hua, WANG Xiao-yan, GAO Yuan. Optimal capacity configuration of grid-connected Wind-PV-storage hybrid power generation system [J]. Journal of Power System and Automation, 2019, 31(10): 59−65. DOI: 10.19635/j.cnki.csu-epsa.000127. (in Chinese)

(Edited by ZHENG Yu-tong)

中文导读

考虑 V2G 影响的光伏电动汽车充电站多目标容量配置优化方法

摘要：大量电动汽车接入微电网将带来很多问题。本文在考虑 V2G 的情况下，提出了两种充放电模式，构建了基于出行习惯的无序充放电模式和考虑峰谷电价的有序充放电模式的电动汽车充放电负荷模型，运用蒙特卡罗法对实例进行仿真验证。在基于 V2G 的两种不同充放电模式下，建立以能源利用率最大化和系统投资、运行成本最小化为目标函数的数学模型，给出了决策变量范围，功率平衡要求的约束条件及能量交换策略。运用 NSGA-II 和 NSGA-SA 算法对实例分别进行仿真验证。通过对比两种不同模式的仿真结果，证明了考虑 V2G 的有序充放电模式在缓解电网压力、减少系统投资、提高能源效率等方面明显优于无序充放电模式。

关键词：V2G；容量配置优化；峰谷电价；多目标优化；NSGA-II 算法；NSGA-SA 算法